Chiral Recognition of a Synthetic Peptide Using Enantiomeric Conjugated Polyelectrolytes and Optical Spectroscopy

K. Peter R. Nilsson,*,† Johan D. M. Olsson,‡ Franz Stabo-Eeg,§ Mikael Lindgren,§ Peter Konradsson,‡ and Olle Inganäs†

Biomolecular and Organic Electronics, IFM, Linköping University, SE-581 83 Linköping, Sweden, Department of Chemistry, IFM, Linköping University, SE-581 83 Linköping, Sweden, and Department of Physics, The Norwegian University of Science and Technology, 7491 Trondheim, Norway

Received June 7, 2005; Revised Manuscript Received June 9, 2005

ABSTRACT: The synthesis of two chiral isomers of 3-substituted polythiophenes, with cationic side-chain functionalities, and their use as conformational sensitive optical probes for the recording of pH-induced conformational changes in a synthetic peptide are reported. The conformational changes of the synthetic peptide gives rise to geometrical changes of the conjugated polyelectrolytes, and these changes are shown as alterations of the absorption-, emission-, two-photon excitation emission and circular dichroism spectra of the conjugated polyelectrolytes. Interaction between a four-helix bundle conformation of the peptide and the conjugated polyelectrolytes will lead to a more planar conformation of the polyelectrolyte backbone and separation of polyelectrolyte chains, observed as a red shift and an increase of the emitted light from conjugated polyelectrolyte. As the peptide adopts a random-coil conformation, the intensity of the emitted light is further red shifted and the intensity is decreasing, associated with aggregation of the polyelectrolyte chains. Moreover, it is demonstrated how the specific chiral recognition can be quantified as differences in fluorescence emission based on both single- and two-photon excitation from the two enantiomeric isomers which interact differently with the peptide.

Introduction

Conjugated polyelectrolytes (CPs) that are capable of continuously and selectively detecting biological processes have large potential for being used as biosensors and in biomolecular devices. In particular, CPs have been used to detect biospecific interactions through their impact on the conditions for photoinduced charge or excitation transfer[1−9] or through the conformational alterations of the polyelectrolyte chains.[10−13] Recent studies[14−18] have also shown that CPs can be used as novel optical tools for the detection of conformational changes of biomolecules. The conformational flexibility of conjugated polyelectrolytes allow direct connection between the geometry of chains and the resulting electronic structure and processes. If conformational changes of biomolecules lead to alternative conformations of the polyelectrolyte backbone, a change of the absorption and emission properties from the polyelectrolyte is observed.

Chiral conjugated polymers are also of great interest, due to their potential for being used in optoelectronic devices, biosensors, and as artificial enzymes. Especially, polythiophenes[19−26] with an optically active substituent in the 3-position have been studied for these purposes. Chiral polythiophenes normally exhibit optical activity in the $\pi-\pi^*$ transition region, derived from the main-chain chirality when the polymer chains are forming supramolecular, π-stacked self-assembled aggregates in a poor solvent or at low temperature, whereas they demonstrate no activity in the UV−vis region in a good solvent or at high temperatures.[23,27−30] Recent studies,[31−33] using achiral CPs that become optically active upon addition of a chiral guest, show that chirality introduction can also be a result of an acid−base complexation between the CP and the chiral guest. The CPs are forming a one-handed helical structure with a preferred twist, which reflects the stereochemistry of the chiral guest.[31−33]

Natural biopolymers, such as proteins, frequently alter their conformations due to different external stimuli and commonly have one-handed helical conformations that contribute to the three-dimensional ordered structure and the specific function of the biopolymer. The preferable twists of the helical conformations are caused by homochirality of their components (D-sugars and L-amino acids). Normally a polypeptide made from L-α-amino acid residues forms a right-handed helix, and the exclusive one-handed helical conformation is of great importance, as the stereochemistry of biomolecules are widely used to create biospecific interactions and the specificity of enzymatic reactions.

Previous studies[11,14,16,22,26,34,35] of a polythiophene, with a free L-amino acid side chain, poly(3-[(S)-5-amino-5-carboxyl-3-oxapentyl]-2,5-thiophenylene hydrochloride), L-POWT, or a free D-amino acid side chain, poly(3-[(R)-5-amino-5-carboxyl-3-oxapentyl]-2,5-thiophenylene hydrochloride), D-POWT, have shown pH-dependent optical phenomena due to different electrostatic interactions and hydrogen-bonding patterns within the polymer chain and between adjacent polymer chains. The polyelectrolytes adopt a right-handed helical form or a left-handed helical form, depending on the nature of the enantiomeric substituents. The circular dichroism (CD) spectra for the two polyelectrolytes are mirror images, so apparently the nature of the amino acid side chain is reflected in the helical conformation of the polymer backbone.[26]

* To whom correspondence should be addressed. E-mail: petni@ifm.liu.se.
† Biomolecular and Organic Electronics, Linköping University.
‡ Department of Chemistry, Linköping University.
§ The Norwegian University of Science and Technology.

10.1021/ma051188f CCC: $30.25
Published on Web 07/14/2005

Scheme 1[a]

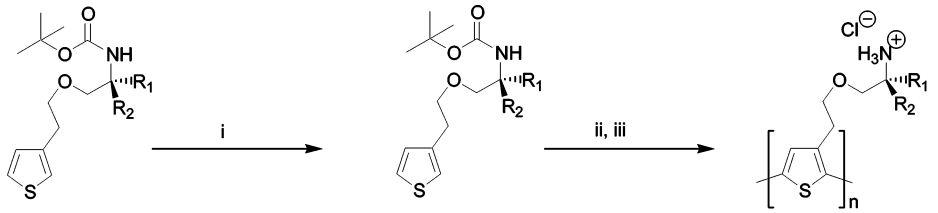

[a] Key: (i) MeI, Ag_2O, CH_2Cl_2, 75 %. (ii) CH_2Cl_2/TFA (4:1), quant. (iii) $FeCl_3$, TBA-OTf, $CHCl_3$, 65 %.

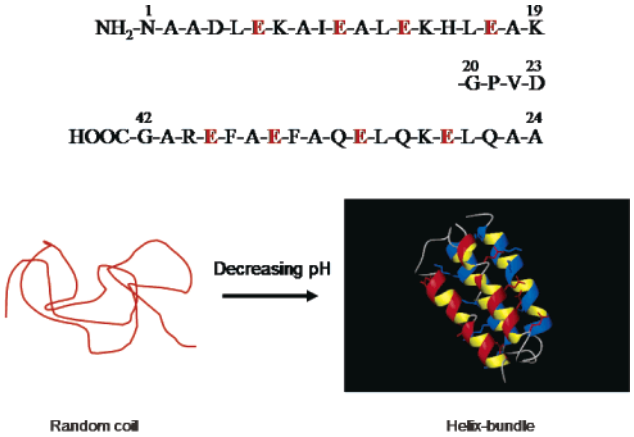

Figure 1. Sequence of JR2E (top) and schematic drawing of the pH-induced conformational changes of the peptide (bottom).

In this article, we report the synthesis of two novel cationic polythiophenes with enantiomeric substituents, poly (3-[(R)-5-amino-5-methoxycarboxyl-3-oxapentyl]-2,5-thiophenylene hydrochloride), D-POMT, and poly (3-[(S)-5-amino-5-methoxycarboxyl-3-oxapentyl]-2,5-thiophenylene hydrochloride), L-POMT, (see Scheme 1). The chiral isomers are used as conformation-sensitive optical probes for the detection of pH-induced conformational changes within a synthetic peptide, JR2E (Figure 1), and a variety of optical spectroscopy techniques are used to demonstrate the unique and selective interaction between the two enantiomeric forms of the chiral polythiophene derivative and the different conformations of the synthetic peptide.

Experimental Section

General Methods. All dry solvents were collected onto 4A predried molecular sieves (Merck). Thin-layer chromatography (TLC) was carried out on 0.25-mm precoated silica gel plates (Merck silica gel 60 F254) and detected by UV absorption (254 nm) and/or by charring with PAA-dip (ethanol/sulfuric acid/*p*-anisaldehyde/acetic acid 90:3:2:1) followed by heating to ~250 °C. FC means flash column chromatography using silica gel (MERCK 60 (0.040−0.063 mm)). ^{1}H and ^{13}C NMR spectra were performed on a Varian Mercury 300 MHz instrument at 25 °C. Chemical shifts are given in ppm relative to trimethylsilane in $CDCl_3$ (δ 0.00) for ^{1}H and ^{13}C or CD_3OD (δ 3.31) for ^{1}H. Optical rotation was recorded at room temperature with a Perkin-Elmer 141 polarimeter, and IR spectra were recorded on a Perkin-Elmer SPECTRUM 1000 FT-IR spectrometer as KBr pellets.

Methyl-((*S*)-2-*tert*-Butoxycarbonylamino-3-(2-thiophen-3-yl-ethoxy))-propionate (2a). To a solution of **1a** (0.846 g, 2.69 mmol) in CH_2Cl_2 (30 mL), MeI (3.75 mL, 40.4 mmol) and Ag_2O (0.81 g, 3.50 mmol) were added. After stirring at 30 °C for 60 h in darkness, the mixture filtered through Celite and concentrated. FC (T/E 12:1) gave **2a** (0.67 g, 2.03 mmol, 75%) as a colorless oil. The (*R*)-enantiomer (**2b**) was synthesized using same protocol as for **2a**. IR and NMR spectra for **2b** were in accordance with **2a**.

R_f = 0.57 (toluene/EtOAc 4:1).

$[\alpha]_D$ = −2.9 (*c* 2.0, $CHCl_3$). (For the synthesized (*R*)-enantiomer (**2b**), $[\alpha]_D$ = +3.0 (*c* 2.0, $CHCl_3$).)

IR ν_{max} cm^{-1}: 636, 666, 779, 1163, 1503, 1715, 2931, 2978, 3103, 3359.

^{13}C NMR ($CDCl_3$) δ: 27.9 (3C), 29.0, 53.6, 58.7, 64.8, 72.0, 79.3, 121.2, 125.2, 127.8, 137.4, 155.1, 170.2.

^{1}H NMR ($CDCl_3$) δ: 1.44 (s, 9H), 2.96 (t, 2H, J = 6.9 Hz), 3.26 (s, 3H) 3.55 (dd, 1H, J = 3.3, 9.3 Hz), 3.72 (dd, 1H, J = 3.3, 9.3 Hz), 4.34 (m, 3H), 6.95 (dd, 1H, J = 5.1, 1.2 Hz), 7.02 (dd, 1H, J = 3.0, 1.2 Hz), 7.23 (dd, 1H, J = 5.1, 3.0 Hz).

L-POMT (3a). 2a (0.36 g, 1.10 mmol) was dissolved in CH_2Cl_2/TFA (4:1, 10 mL). The reaction was quenched after 1 h by adding MeOH (2 mL) and co-concentrated with toluene. The ammonium salt and TBA-OTf (0.54 g, 1.37 mmol) were dissolved in dry $CHCl_3$ (9 mL), and the solution was cooled to 10 °C. Anhydrous $FeCl_3$ (0.80 g, 4.95 mmol) was added to the solution under Ar atmosphere. After it was stirred for 14 h at room temperature, the reaction was quenched with H_2O and diluted with $CHCl_3$. The organic layer was washed with H_2O (2 × 4 mL). The aqueous solution was diluted with acetone (70 mL), and concentrated HCl was added dropwise until the polymer precipitated. After 2 h, the mixture was centrifuged (4 min/2500 rpm). The red salt was washed with acetone (2 × 35 mL), dissolved in H_2O, and reprecipitated from acetone/concentrated HCl. The washing procedure was repeated twice to give **3a** (0.19 g, 0.72 mmol, 65%) as a red salt. The (*R*)-enantiomeric form of the polyelectrolyte (**3b**, D-POMT) was synthesized using same protocol as for **3a**. IR and ^{1}H NMR spectra for **3b** were in accordance with **3a**.

IR ν_{max} cm^{-1}: 968, 1101, 1234, 1504, 1591, 1742, 2879, 3344.

^{1}H NMR (CD_3OD) δ: 3.07 (bs, 2H)*, 3.34 (s, 3H)*, 3.83 (bs, 2H), 4.33 (bs, 1H), 4.59 (bs, 2H), 7.37 (bs, 1H).

The asterisk indicates a peak partly hidden in MeOH (δ 3.31).

Matrix-Assisted Laser Desorption/Ionization Time-of-Flight Mass Spectroscopy (MALDI-TOF-MS). An aqueous solution of the polyelectrolyte (50 μL) and 50 μL of α-cyano-4-hydroxy-*trans*-cinnamic acid (CHCA) in 0.1% TFA/acetonitrile (1:1) were coevaporated on a target plate. The spectra were recorded in linear-positive mode with a Voyager-DE STR Biochemistry Workstation.

Spectroscopic Experiments. A stock solution containing 3.0 mg of polyelectrolyte mL^{-1} (L-POMT or D-POMT) in deionized water was prepared and placed on a rocking table for 1 h. The following buffer solutions were prepared:

20 mM Na citrate (pH 2.5), 20 mM MES (pH 5.9), 20 mM Na-phosphate (pH 6.8), and 20 mM Na-carbonate (pH 10.0). All the chemicals used were of analytical grade.

For the absorption, emission, and CD measurements, 15 μL of the polyelectrolyte stock solution was diluted with 30 μL of the negatively charged peptide (JR2E)[14] solution (2.2 mg mL^{-1}) and diluted with one of the buffer solutions to a final volume of 1200 μL, and the sample was placed on a rocking table for 1 h before the spectrum was recorded. The procedure was repeated for all the buffer systems and the different enantiomeric forms of the polyelectrolytes. Optical spectra were

recorded on a Perkin-Elmer Lambda 9 UV/VIS/NIR spectrophotometer for UV/VIS, a Hitachi F4500 fluorescence spectrophotometer for fluorescence, and an I.S.A. Jobin-Yvon CD6 (5 mm quartz cell) for CD.

Time-Resolved Fluorescence Experiments. Time-resolved fluorescence decays were recorded using an IBH 5000 U fluorescence lifetime spectrometer system with 1-nm resolved excitation and emission monochromators (5000M). The system was equipped with a TBX-04 picosecond photon-detection module. An IBH NanoLED-10 (443 nm) was used as excitation source for decay measurements of single-photon excitation. A spectrometer port without a monochromator was used, and a Melles Griot colored glass filter (FCG 067) was used to block scattered light from the excitation source. The fluorescence lifetime decays were measured using time-correlated single-photon counting (TC-SPC) along with the IBH Data Station v 2.1 software for operation of the spectrometer and deconvolution and analysis of decays. The DAQ card settings were chosen to give a time resolution below 10 ps.

Two-Photon Absorption-Induced Fluorescence Experiments. A Coherent Mira 900 with a femtosecond cavity in conjunction with a Coherent 9200 Pulse-Picker was used as an excitation source. The pulse picker is beneficial since it lowers the high pulse repetition frequency of the MIRA 900 giving essentially the same peak-power of individual pulses. Hereby it is suitable for multiphoton excitation, avoiding heating or other irreversible changes of the sample. Moreover, by carrying out control experiments at different (lower) pulse repetition frequency one also avoids spurious results that might be caused by, e.g., incoherent excited-state absorption processes. The pulses of the used fundamental tone at 886 nm were 170 fs long, and typically 44-mW output was generated at a pulse repetition frequency of 4.75 MHz set to the pulse picker. This repetition rate also allows for convenient and rapid detection of the fluorescence decay time using the single-photon counting technique. The laser beam was directed into one of the open ports of the time-resolved spectrometer allowing time-resolved decay measurements as well as recording of the emission spectrum by scanning the monochromator in front of the PMT detector. The excitation beam was linearly polarized. However, the detection of the fluorescence emission was carried out without a polarizer. A series of three lenses was used to first expand the laser beam and finally focus it into the center of the 1-cm standard quartz cuvette used for fluorescence measurements. A Newport hot mirror was used to block scattered light from the excitation source. No attempts were made to calibrate the detector or monochromator wavelength dependence since they were essentially flat according to specifications. As a reference time point, a fraction of the light from the pulse picker was separated with a glass plate and projected onto an IBH TBX-01 optical trigger.

Results and Discussion

Synthesis. Ag_2O and MeI converted the already synthesized serine-substituted thiophene derivatives **1a**[22] and **1b**[26] to the corresponding methyl ester, and the Boc-groups were removed in CH_2Cl_2/TFA to give the ammonium salts readily for polymerization. Polymerization was performed by a method reported by Sugimoto et al.[36,37] using chemical oxidation with anhydrous $FeCl_3$. The water-soluble polyelectrolytes were then precipitated by adding acetone and concentrated hydrochloric acid, washed with acetone, and dried to achieve **3a** (L-POMT) and **3b** (D-POMT) as red powders (Scheme 1).

Lately, MALDI-TOF-MS has been developed as a powerful tool when analyzing synthetic polymers, both for chain-length studies and for end-group analysis of different polymers. Different techniques considering the use of matrix, cationization agents, and the matrix/analyte ratio have also been investigated.[38,39] The use of MALDI-TOF-MS for characterization of water-soluble thiophene polymers using same conditions (matrix, mode, etc.) has earlier showed to be a fruitful characterization method.[26]

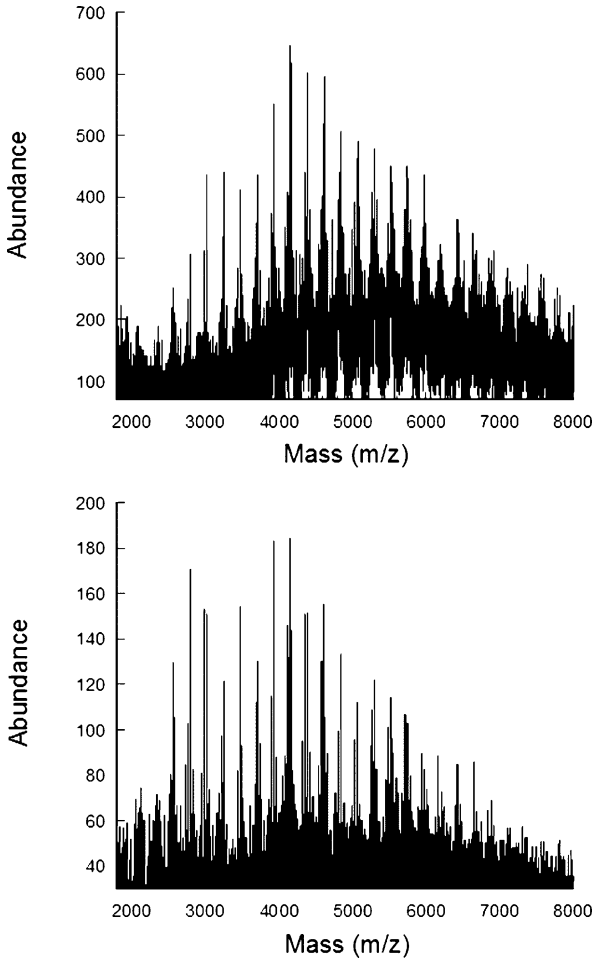

Figure 2. MALDI-TOF-MS spectra of L-POMT (top) and D-POMT (bottom) showing the chain length distribution recorded in a linear positive mode using CHCA as matrix.

The length of the thiophene backbones in the polyelectrolytes were elucidated by MALDI-TOF-MS. The MALDI-TOF spectra (Figure 2) from the polymer showed a molecular weight distribution mainly between 2500 and 6000 following ion series corresponding to $[228n + 35]^+$ and $[228n + 70]^+$ (Figure 2). The spectra correspond to polyelectrolytes containing between 11 and 26 thiophene units in the backbone. Adducts of 35 and 70 originate from one or two covalently bound chlorine atoms, respectively. The chlorine adducts are believed to originate from the oxidizing agent in the polymerization, $FeCl_3$, which are known to give impurities of iron or chlorine[40] and are in accordance both with previous result from our group and a report published by McCarley et al.[41] Hence, the ion series $[228n + 35]^+$ and $[228n + 70]^+$ corresponds to substituted thiophene (ST) units and one or two chlorine atoms, $[STn + Cl]^+$ or $[STn + 2Cl]^+$ where n is the number of ST in the backbone. By conversion of the carboxyl group of the earlier synthesized zwitterionic polyelectrolyte POWT,[22,26] with 13−19 thiophene units in the backbone, to the corresponding methyl ester, we decrease the polarity of the polyelectrolyte. The increased length of the backbone (11−26 ST) is believed to originate from the increased solubility of the less polar side chain of POMT (compared to POWT) in the polymerization, performed in $CHCl_3$.

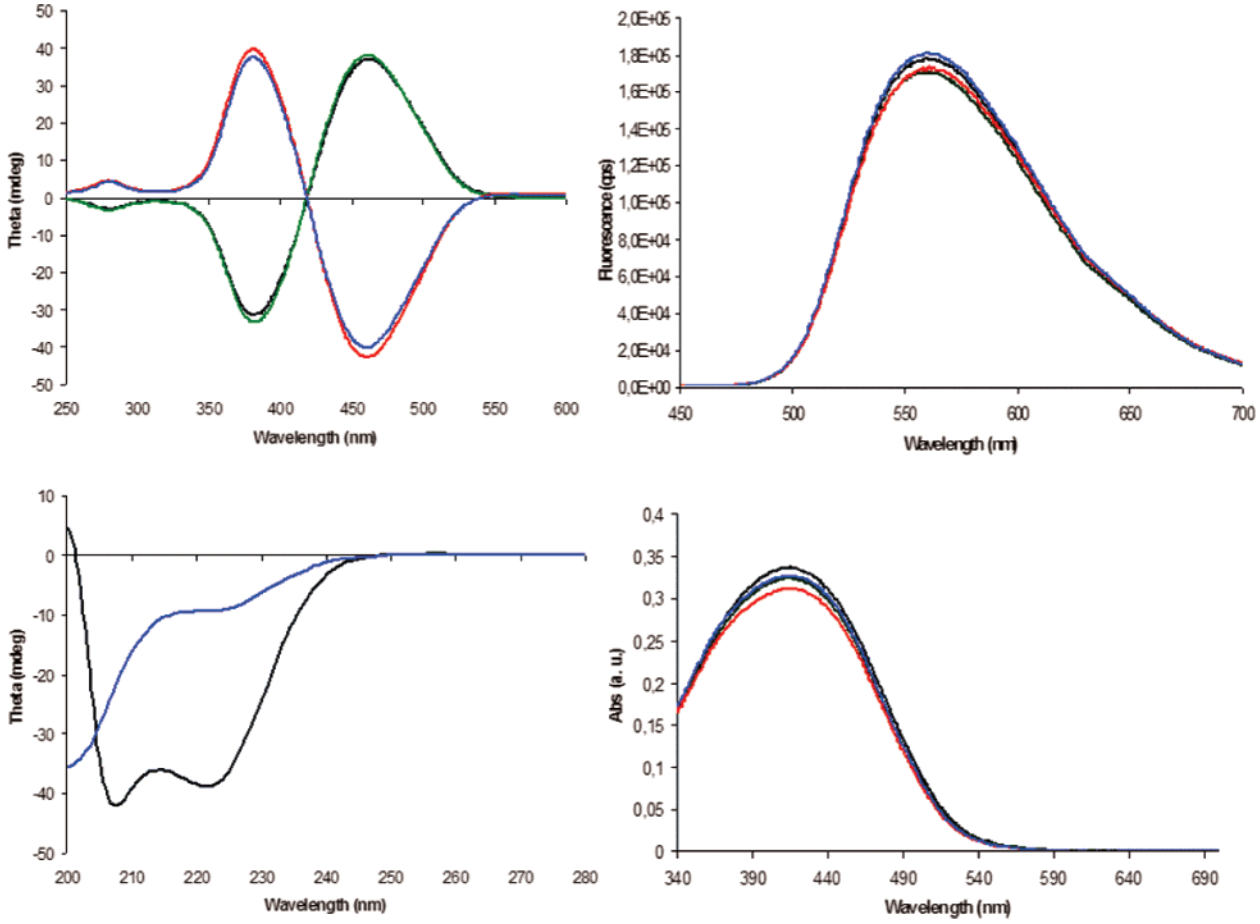

Figure 3. CD spectra (top left), fluorescence spectra (top right), and absorption spectra (bottom right) of 10 μM L-POMT in 10 mM MES pH 5.9 (black line) or 10 mM Na phosphate pH 6.8 (green line) and 10 μM D-POMT in 10 mM MES pH 5.9 (red line) or 10 mM Na phosphate pH 6.8 (purple line). CD spectra (bottom left) of 10 μM JR2E in 10 mM MES pH 5.9 (black line) or 10 mM Na phosphate pH 6.8 (purple line).

Optical Measurements. A detailed photophysical characterization for L-POMT in different buffer solutions in the range 2.5−10 was carried out. This included determination of extinction coefficient, fluorescence quantum yield, as well as the two-photon absorption (TPA) cross section. All these photophysical parameters were found to depend strongly on the pH. The extinction coefficients were found to be ϵ(pH 2.5) = 30 mg/L·cm, ϵ(pH 5.9) = 22 mg/L·cm, and ϵ(pH 10) = 15 mg/L·cm. The quantum efficiency was determined plotting the absorbance vs the integrated fluorescence yield using fluorescein as a reference.[42] The fluorescence quantum yield at the three different pH values 10, 5.9, and 2.5 was found to be 0.03, 0.07, and 0.10, respectively. By use of an identical concentration of fluorescein in ethanol as a reference, the TPA cross section at three different pHs, 10, 5.9, and 2.5, was estimated to be 82, 140, and 310 GM (Göppert−Mayer; e^{-50} cm s/photon), respectively, by comparing the two-photon induced fluorescence emission and adjusting for the differences in fluorescence quantum yield.[43] Hence, the TPA cross section of POMT at pH 2.5 is approximately 10 times that of fluorescein (ethanol) at 800-nm excitation. The pronounced maximum at low pH indicates that the polythiophene takes a more planar conformation. The detailed results and discussions of these measurements will appear elsewhere (Stabo-Eeg et al., in preparation); here only the experiments relevant for the discussion of the interaction between the two enantiomeric forms of POMT and the synthetic peptide will be discussed.

The absorption spectra for L-POMT and D-POMT in different buffer solutions are shown in Figure 3. In the pH range 5.9−6.8, the polyelectrolytes have absorption maxima of 412 nm, associated with a nonplanar conformation of the polyelectrolyte backbone. Previous studies[26,35] of similar polyelectrolytes with zwitterionic side chains have shown a pH-induced yellow to orange color change in the same pH interval, indicating that the methylation of the carboxyl groups L-POMT and D-POMT is changing the pH induced behavior previously seen for the zwitterionic polyelectrolytes. As the anionic carboxyl groups are methylated, the cationic amine groups are the only groups that can be protonated or deprotonated in water solution. The cationic amine groups have most likely a high pK_a value (9.21 for the amine group of serine), and these groups are preferably in the protonated form in the pH range 5.9−6.8. The absorption maxima from L-POMT and D-POMT are similar, so the altered stereochemistry of the chiral center on the side chain is not affecting the absorption properties of the polyelectrolyte backbone. This result is in agreement with an earlier study,[26] where isomers of a zwitterionic polythiophene derivates were evaluated.

The emission spectra for the enantiomeric forms of the polyelectrolytes in the pH range 5.9−6.8 are also similar (Figure 3). An emission maximum of 563 nm is associated with a generally nonplanar conformation of the polyelectrolyte backbone and separation of the polyelectrolyte chains, in agreement with the results

from the absorption measurements. However, there is a shoulder at longer wavelength and earlier studies[34,35] of a similar polyelectrolyte have shown that this shoulder might be associated with an interchain emission process. Thus, there is most likely some contact between the polyelectrolyte chains as a shoulder in the emission spectrum is observed for all of the polyelectrolyte solutions. In concurrence with the absorption measurement, the altered chirality of the polyelectrolyte side chains does not seem to influence the emission properties from the polyelectrolyte chains.

As previously reported,[19−25] optically active PTs exhibit a split-type induced CD (ICD) in the $\pi-\pi^*$ transition region. This ICD is accompanied by a color change from yellow-orange to purple and a decreased intensity of the emitted light, which relates to a transition from a disorded coil-like form to a rodlike, π-stacked one in order to give a chiral supramolecular aggregate with interchain interactions of transoidal polythiophenes. The CD spectra of L-POMT and D-POMT after 10 min of incubation in different buffer solutions are shown in Figure 3. The conjugated polyelectrolytes display a split-type ICD in the $\pi-\pi^*$ transition region. However, in this case, the ICD is most likely a result of main-chain chirality, such as a predominantly one-handed helical structure induced by the chiral nature of the side chains of the CPs,[15,22,26,31−33,35] as the ICD is accompanied with a blue-shifted absorption and an increase of the emitted light. The results, blue-shifted absorption and increased emission intensity with induced helicity, have previously been reported for the unmethylated zwitterionic polythiophene derivative,[26] supporting the explanation of a predominantly one-handed helical structure. The CD spectra show that the magnitude of the Cotton effect for the CPs is similar in this pH interval (5.9−6.8) and the shape and the sign of the ICD pattern for the two CPs are mirror images, indicating that the altered chirality of the polymer side chain is influencing the helical twist of the polyelectrolyte backbone. Similar results were recently reported for a zwitterionic polythiophene with enantiomeric substituents,[26] and the shape and sign of the ICD pattern are characteristic of a right-handed or left-handed helical form of polythiophene.[22,26,28,29,35] The CD spectra for L- and D-POMT also show a minor peak at approximately 280 nm, which is associated with the absorption of the thiophene ring. This peak has also opposite signs for the polyelectrolytes, indicating that the chirality of the thiophene backbone is different for the two polymers.

The CD spectrum (Figure 3) in the far UV region for JR2E at pH 5.9 shows strong negative peaks at 208 and 222 nm, indicative of a helical structure. At pH 6.8, the CD spectra for JR2E (Figure 3) is altered and a strong negative peak around 200 nm and a weak negative peak at 223 nm, indicative of a random coil or a β-like structure, are observed. The JR2E sequence was designed to form a heterodimeric four-helix bundle motif upon addition of a positively charged peptide,[14] and the CD spectra at higher pH shows that no homodimeric four-helix bundles are formed due to electrostatic repulsion between the negatively charged glutamate (E) groups. As the pH is decreased (5.9), the glutamate residues become protonated and homodimeric four-helix bundles are allowed to form as the negative charge of the peptide is removed. The helical motif is most likely stabilized by hydrophobic interactions between the nonpolar amino acids and the hydrogen bonding between the glutamate groups of the peptide. A schematic drawing of the pH-induced conformational changes of JR2E is shown in Figure 1.

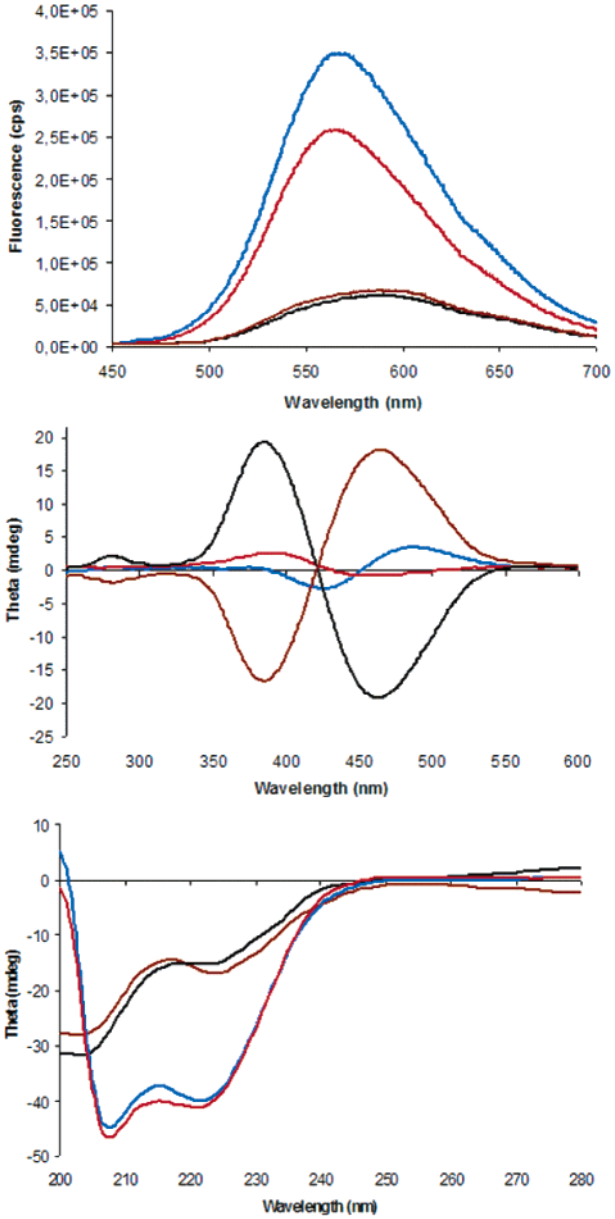

Figure 4. Fluorescence spectra (top), CD spectra (middle and bottom) of 10 μM L-POMT in 10 mM MES pH 5.9 with 10 μM of JR2E (blue line) or in 10 mM Na phosphate pH 6.8 with 10 μM of JR2E (brown line), and 10 μM D-POMT in 10 mM MES pH 5.9 with 10 μM of JR2E (red line) or 10 mM Na phosphate pH 6.8 with 10 μM of JR2E (black line).

The CD spectra of the two polyelectrolytes mixed with JR2E in 20 mM Na phosphate pH 5.9 buffer solutions are shown in Figure 4. The CD spectra in the far-UV region are not altered, indicating that the peptide adopts a similar helical structure, whether the polymer is present or not. On the other hand, the split-type ICDs from the polymer backbone in the $\pi-\pi^*$ transition region are greatly reduced upon addition of JR2E, clearly showing that an interaction between the polyelectrolytes and the peptide occurs. The minor peak at approximately 280 nm, which is associated with the absorption of the thiophene ring, has also vanished. The absorption maxima (Table 1) of L-POMT and D-POMT are also red shifted upon interaction with JR2E, suggesting that the polyelectrolyte backbones adopt more

Table 1. Absorption and Emission Maxima for L-POMT, D-POMT, L-POMT/JR2E, and D-POMT/JR2E at Different pHs

sample	absorption max (nm)	emission max (nm)
L-POMT pH 5.9	412	563
D-POMT pH 5.9	412	563
L-POMT pH 6.8	412	563
D-POMT pH 6.8	412	563
L-POMT/JR2E pH 5.9	426	568
D-POMT/JR2E pH 5.9	426	565
L-POMT/JR2E pH 6.8	425	592
D-POMT/JR2E pH 6.8	425	592

planar conformations due to the interaction with the peptide. However, the CD spectra of the polyelectrolytes are not mirror images, indicating that alternative interactions between the peptide and the polyelectrolyte occur depending on the stereochemistry of the cationic side chains and/or the chirality of the backbone of the CP.

The emitted (Figure 4, Table 1) light of the polyelectrolytes are also altered upon interaction with the helical form of the peptide. The polyelectrolytes emit light with slightly longer wavelength, and the intensity of the emission is increased, suggesting that the interactions between the helical peptide and the polyelectrolytes are leading to more planar polyelectrolyte backbones and separation of polymer chains. The absorption maxima of the polyelectrolytes are also red shifted (Table 1), clearly showing that the backbones of the conjugated polyelectrolytes become more planar upon interaction with the peptide. Apparently, the emitted light from L-POMT is slightly more red shifted and has a higher intensity than the light emitted from D-POMT, suggesting that the backbones for the two polyelectrolytes are to some extent adopting different conformations. These results are in agreement with the results from the CD measurement, demonstrating that the stereochemistry of the cationic side chains and/or the chirality of the CP backbones are forcing the two polyelectrolytes to interact differently with the peptide. All of the optical data also suggest that the peptide has a rigid structure at pH 5.9 and that the polyelectrolytes adapt their conformations to the helical peptide structure. The backbone conformations of the polyelectrolytes are most likely slightly different, due to the fact that the CPs will adapt differently to the right-handed helical form of the peptide. It would be of great interest to synthesize a peptide containing D-amino acids to see if the optical phenomena are reversed and such work is in progress.

Upon mixing of the peptide and the polyelectrolytes in 20 mM Na phosphate pH 6.8 buffer solutions the optical data from the molecules (Figure 4) are altered compared with the data seen for the pure peptide and the pure polyelectrolyte solutions (Figure 3). The CD spectra of the peptide in the far-UV region are altered, indicating that the peptide adopts slightly different structures when the polyelectrolyte is present or not. The CD spectra for JR2E mixed with the polyelectrolytes at pH 6.8 (Figure 4) have a strong negative peak around 202 nm and a peak at 222 nm, indicative of a random-coil structure with some helical content. These results show that an interaction between the polymers and the peptide occurs and that the polyelectrolytes most likely induce some helical structure in the peptide. However, the helical content in the peptide is not as high as seen for the peptide at pH 5.9, where homodimeric four-helix bundles are formed. Interestingly, the peak at 222 nm is most abundant as the peptide is interacting with L-POWT, suggesting that the enantiomeric substituents of the CP side chains are inducing different conformations in the synthetic peptide. It is probably easier for L-POMT to induce a right-handed helical conformation in the peptide, as L-POMT adopts a right-handed helical form of polythiophene.

The CD spectra of the polyelectrolytes are also altered upon interaction with the peptide. The ICDs are decreased, suggesting that the backbone of the conjugated polyelectrolytes become more planar, and this is also seen in the absorption measurements, as the absorption maxima for the CPs are red shifted. The absorption maxima are similar and the CD spectra are mirror images, indicating the backbones of L-POMT and D-POMT are adopting comparable conformations. On the other hand, the ICDs are more intense than the ICDs observed for the polyelectrolytes interacting with the peptide at pH 5.9 and the minor peak at approximately 280 nm are also observed. These observations suggest that the backbone of the polyelectrolytes are adopting a more planar conformation upon interaction with the random-coil conformation of the peptide and a less planar conformation when interacting with the helical form of the peptide. The data from the CD measurements clearly shows that both the peptide and the CPs alters their conformation upon interactions, in contrast to the result obtained with solution at more acidic pH where the CPs adopt their conformation to the structure of the peptide.

The emission spectra (Figure 4) for the polyelectrolytes are also altered upon interaction with the peptide at pH 6.8. The polyelectrolytes emit light with longer wavelength, emission maximum of 592 nm, and the intensity of the emission is decreased, suggesting that the interactions between the peptide and the polymers are leading to more planar polyelectrolyte backbones and to aggregation of the polyelectrolyte chains. A shoulder at longer wavelengths in the absorption spectra (see figure S1 Supporting Information), associated with aggregation of polyelectrolyte chains, is also observed. The emission maximum, 592 nm, and the emission spectra are identical for the two polyelectrolytes, in agreement with the result from the CD measurements that the backbones of the polyelectrolytes have similar conformation. However, the emission spectra of the CPs interacting with the helical or the random-coil conformation of the peptide are considerably different, signifying the use of CPs as conformation sensitive optical probes.

More indications of specific interactions between the polymer and the peptide were implied by the results of time-resolved fluorescence studies. Decay time traces obtained from the sole polymers and peptide complexes at pH 5.9, using time-correlated single photon counting, are shown in Figure 5 along with the decay trace representing the response of the detection system. The displayed emission decays are obviously not single exponentials, as we may expect from polymers of various lengths and a distribution of more or less different conformations. The case L-POMT/JR2E (green curve) is distinctly different from all the other decay traces. By assumption of a linear combination of three monoexponential decays one of the decay times is always determined very short, in the range 5−9 ps, contributing 25−40% of the total amplitude for all cases. This is also

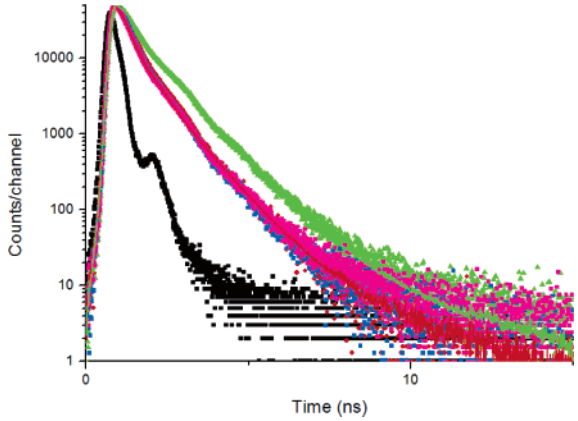

Figure 5. TC-SPC decay traces of L and D forms of the polyelectrolyte along with complexes with peptides (LP and DP) in 10 mM MES pH 5.9. L-POMT/JR2E (green triangles); D-POMT/JR2E (purple squares); L-POMT (blue squares); D-POMT (blue squares). Excitation is 443 nm for all cases. Emission is at 560 nm for L and D and at 580 nm for LP and DP. The black squares are a trace from instrument response, and solid lines are fits as described in the text and in Table 2.

Table 2. Summary of the Two Slowest Time Decay Parameters Obtained by Assuming a Linear Combination of Three Monoexponential Decays[a]

D-POMT/JR2E	L-POMT/JR2E	L-POMT	D-POMT
$\tau1 = 0.31$ (36%)	$\tau1 = 0.35$ (36%)	$\tau1 = 0.31$ (36%)	$\tau1 = 0.30$ (37%)
$\tau2 = 0.89$ (25%)	$\tau2 = 0.94$ (25%)	$\tau2 = 0.82$ (27%)	$\tau2 = 0.84$ (26%)

[a] L-POMT, D-POMT, L-POMT/JR2E, and D-POMT/JR2E at pH 5.9. Time is nanosseconds, and the relative amplitude is given in parentheses after each decay time.

approximately the limit of resolution of our detection system, and hence, this decay time parameter is regarded as the "instantaneous" emission in view of the time frame of our measurements.

The remaining two decay parameters for the four cases are summarized in Table 2. The parameters obtained for the sole L and D forms are identical within experimental uncertainty; however, both decay parameters for the peptide complexes are the same or larger. The overall decay time of the complex L-POMT/JR2E is larger as both the decay parameters and the relative weight of the slower component are distinctly larger, as one can judge from the appearance of the traces in Figure 5. Thus, the time-resolved results support the findings from steady-state fluorescence emission spectra and CD spectra discussed above.

Fluorescence emission based on multiphoton absorption processes can give an additional dimension of selectivity.[44−46] The TPA process has different selection rules and is in additional strongly polarization dependent,[47] being a technique with capability to discern different chiral and nonchiral conformations. The characterization of TPA cross sections from fluorescence emission and used of TPA in laser confocal microscopy was recently reviewed by Webb and co-workers.[48] Tiophenes and oligomers thereof are predicted to have rather large TPA cross sections, where the effect in general is increased with increased conjugation length.[49] The two-photon induced decay traces for L-POMT at pHs 2.5, 5.9, and 10 are shown in Figure 6. The excitation wavelength was here 830 nm, and the emission was monitored at 575 nm using a 32-nm slit. Essentially the same results were found in the wavelength range 780−850 nm corresponding to half the photon energy associated with the one-photon absorption band (Figure 3).

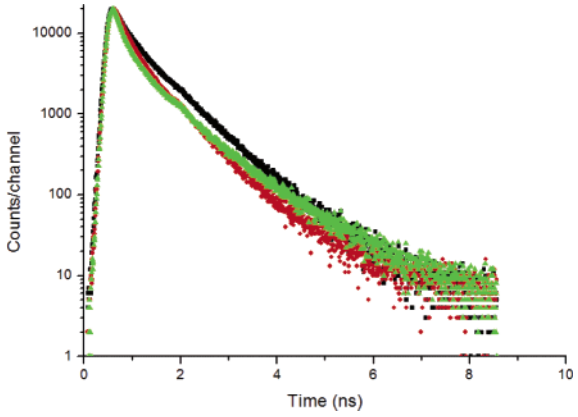

Figure 6. TC-SPC decay traces of L-POMT upon two-photon excitation at 830 nm and at different pH. The emission was recorded at 575 nm using a 32-nm slit: black squares, pH 2.5; red diamonds, pH 5.9; green triangles, pH 10.

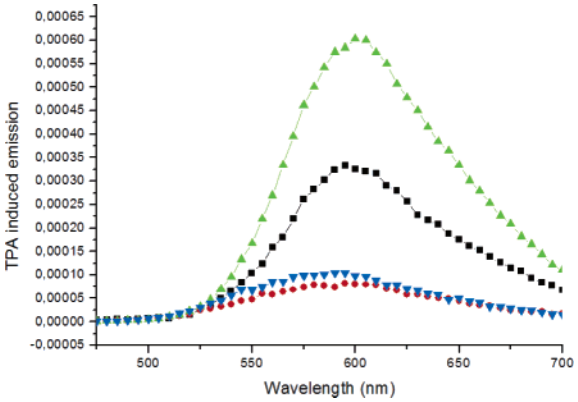

Figure 7. Spectra of two-photon excitation assisted fluorescence emission of L, D, LP, and DP samples in 10 mM MES pH 5.9 upon excitation at 886 nm: L-POMT/JR2E, green triangles; D-POMT/JR2E, black squares; L-POMT, blue triangles; D-POMT, red dots. The data sets are normalized to the area of the fluorescence emission spectrum obtained from single photon excitation at 443 nm.

As the TPA-induced fluorescence resulted in essentially the same time decay traces as found using single-photon excitation, it can be concluded that the emission originates from the same excited state (Figure 5). However, the decays are similar to the one-photon excitation decays (Figure 5) characterized as multiexponential decay times; thus the decay time obtained from curve fittings are difficult to interpret. This originates probably from the complexity of the polymer rendering the photoexcitation and emission processes to occur in several types of microenvironments also for the sole polymer in equilibrium with the solvent. To obtain further evidence on the unique and specific complexation between POMT and JR2E, the corresponding fluorescence emission spectra were recorded using two-photon excitation. The emission yield was found to differ distinctly from the emission yield obtained using single-photon excitation. The emission spectra shown in Figure 7 are all recorded under exactly the same experimental conditions (pulse repetition rate, laser power, sample cell geometry, focusing); however, the collected emission obtained by scanning the monochromator has in each case been normalized to the area of the fluorescence spectrum obtained from the very same solutions using the 443-nm laser diode as (single photon) excitation source. Hereby we minimize differences that might arise due to differences in absolute

polymer concentration, etc. Notably, the two-photon excitation spectra obtained from the complexes are much larger than those of the sole POMT forms, again with the combination L-POMT/JR2E being the most spectacular.

Since multiphoton absorption processes of conjugated polymers can be enhanced[50] and are enhanced in polythiophenes in particular,[49,51] as we increase the conjugation length, we may tentatively conclude that the interaction between the POMT and JR2E in both cases renders the polymer in a more planar form, disrupting the helicity as observed in the sole polymer. This is in accordance with the CD results discussed above, and since the emission upon two-photon excitation was normalized to the emission of the single excitation, we may conclude that two-photon excitation, as represented in Figure 7, gives a more specific signature upon complex formation than the emission detected by single-photon excitation (Figure 4). Moreover, the preliminary photophysical characterization also supports this conclusion since both the quantum yield and extinction coefficient are at their maxima for low pH values, and this coincides with the largest two-photon cross section (Stabo-Eeg et al., in preparation).

The geometry of the polyelectrolyte chains and the optical processes can be tuned differently depending on the conformation of the peptide being used. Previous studies[14−18] have shown that conjugated polyelectrolytes can be used as conformation sensitive probes for conformational changes when proteins or peptides assembles in to different structures. The results report herein show the ability of recording conformational changes within one peptide and offers a wide range of opportunities for the development of conformation sensitive optical biosensors based on CPs. This is of great interest as many diseases are associated with structural abnormalities in proteins. Another possibility is to use polyelectrolytes with enantiomeric substituents and backbones with different chirality for chiral imaging of biomolecules in tissue samples. The different isomers of the polyelectrolytes are interacting differently with the same peptide depending on the peptide conformation, and this phenomenon might offer a possibility of making a diverse range of conformational sensitive optical biosensors. We here also demonstrated that the polyelectrolyte chains possess multiphoton excitation capability using a femtosecond near-infrared laser as the excitation source, with higher specificity in the chiral recognition than single-photon excitation emission. This facilitates the use of the polyelectrolytes to quantify the presence of peptides and related biomolecules using multiphoton microscopy and related modern photonic tools currently being developed for the bio- and material sciences.

Conclusions

By use of two isomers of a conjugated polythiophene with a cationic side chain, we have showed that CP can be used as conformation-sensitive optical probes for the recording of conformational changes within a synthetic peptide. The two isomers also interact differently with the peptide, due to the stereochemistry of the side chains and the chirality of the backbone. As the peptide adopts a well-defined structure, the CP adopts their conformation to the peptide structure. On the other hand, as the peptide has a random-coil conformation, the CPs induce some well-defined structure in the peptide. It is further shown how multiphoton excitation schemes can be used to detect such conformational states, pointing out novel application areas within laser-based microscopy. Our future efforts in this system will be to determine the different types of interaction forcing the polyelectrolytes to show this extraordinary behavior. It would also be of great interest to combine the different isomers with natural chiral biomolecules to see if the difference in chirality of the conjugated polyelectrolyte will cause a different interaction with the biomolecule of interest and how the technique describe in this article can be used in different types of biosensors.

Acknowledgment. We thank Lars Baltzer and coworkers (Uppsala University, Uppsala, Sweden), for supplying the peptide, JR2E. This work was partially funded by a grant from the Norwegian Research Council within the NanoMat program (Contract #153529/s10) (M.L.) as well as the Swedish Nanotek program (M.L.).

Supporting Information Available: Absorption spectra for the polyelectrolyte/peptide complexes in different buffer solutions. This material is available free of charge via the Internet at http://pubs.acs.org.

References and Notes

(1) Wang, J., et al. *Macromolecules* **2000**, *33*, 5153.
(2) Fan, C.; Plaxco, K. W.; Heeger, A. J. *J. Am. Chem. Soc.* **2002**, *124*, 5642.
(3) Wang, D., et. al. *Proc. Natl. Acad. Sci. U.S.A.* **2002**, *99*, 49.
(4) Gaylord, B. S.; Heeger, A. J.; Bazan, G. C. *Proc. Natl. Acad. Sci. U.S.A.* **2002**, *99*, 10954.
(5) Gaylord, B. S.; Heeger, A. J.; Bazan, G. C. *J. Am. Chem. Soc.* **2003**, *125*, 896.
(6) Liu, B.; Gaylord, B. S.; Wang, S.; Bazan, G. C. *J. Am. Chem. Soc.* **2003**, *125*, 6705.
(7) Kumaraswamy, S.; Bergstedt, T.; Shi, X.; Rininsland, F.; Kushon, S.; Xia, W.; Ley, K.; Achyuthan, K.; McBranch, D.; Whitten, D. *Proc. Natl. Acad. Sci. U.S.A.* **2004**, *101*, 7511.
(8) Xu, Q. H.; Gaylord, B. S.; Wang, S.; Bazan, G. C.; Moses, D.; Heeger, A. J. *Proc. Natl. Acad. Sci. U.S.A.* **2004**, *101*, 11634.
(9) Rininsland, F.; Xia, W.; Wittenburg, S.; Shi, X.; Stankewicz, C.; Achyuthan, K.; McBranch, D.; Whitten, D. *Proc. Natl. Acad. Sci. U.S.A.* **2004**, *101*, 15295.
(10) Ho, H.-A., et. al. *Angew. Chem., Int. Ed.* **2002**, *41*, 1548.
(11) Nilsson, K. P. R.; Inganäs, O. *Nature Mater.* **2003**, *2*, 419.
(12) Ho, H.-A.; Leclerc, M. *J. Am. Chem. Soc.* **2004**, *126*, 1384.
(13) Dore, K.; Dubus, S.; Ho, H.-A.; Levesque, I.; Brunette, M.; Corbeil, G.; Boissinot, M.; Boivin, G.; Bergeron, M. G.; Boudreau, D.; Leclerc, M. *J. Am. Chem. Soc.* **2004**, *126*, 4240.
(14) Nilsson, K. P. R.; Rydberg, J.; Baltzer, L.; Inganäs, O. *Proc. Natl. Acad. Sci. U.S.A.* **2003**, *100*, 10170.
(15) Nilsson, K. P. R.; Rydberg, J.; Baltzer, L.; Inganäs, O. *Proc. Natl. Acad. Sci. U.S.A.* **2004**, *101*, 11197.
(16) Nilsson, K. P. R.; Inganäs, O. *Macromolecules* **2004**, *37*, 9109.
(17) Nilsson, K. P. R.; Herland, A.; Hammarström, P.; Inganäs, O. *Biochemistry* **2005**, *44*, 3718−3724.
(18) Herland, A.; Nilsson, K. P. R.; Olsson J. D. M.; Konradsson, P.; Hammarström, P.; Inganäs, O. *J. Am. Chem. Soc.* **2005**, *127*, 2317.
(19) Lemaire, M.; Delabouglise, D.; Garreau, R.; Guy, A.; Roncali, J. *J. Chem. Soc., Chem. Commun.* **1988**, 658.
(20) Kotkar, D.; Joshi, V.; Ghosh, P. K. *J. Chem. Soc., Chem. Commun.* **1988**, 917.
(21) Roncali, J.; Garreau, R.; Delabouglise, F.; Garnier, F.; Lemaire, M. *Synth. Met.* **1989**, *28*, 341.
(22) Andersson, M.; Ekeblad, P. O.; Hjertberg, T.; Wennerström, O.; Inganäs, O. *Polym. Commun.* **1991**, *32*, 546.
(23) Bouman, M. M.; Havinga, E. E.; Janssen, R. A. J.; Meijer, E. W. *Mol. Cryst. Liq. Cryst.* **1994**, *256*, 439.
(24) Bouman, M. M.; Meijer, E. W. *Adv. Mater.* **1995**, *7*, 385.
(25) Bidan, G.; Guillerez, S.; Sorokin, V. *Adv. Mater.* **1996**, *8*, 157.
(26) Nilsson, K. P. R.; Olsson, J. D. M.; Konradsson, P.; Inganäs, O. *Macromolecules* **2004**, *37*, 6316.
(27) Langeveld-Voss, B. M. W.; Bouman, M. M.; Christiaans, M. P. T.; Janssen, R. A. J.; Meijer, E. W. *Polym. Prepr.* **1996**, *37*, 499.

(28) Langeveld-Voss, B. M. W.; Janssen, R. A. J.; Christiaans, M. P. T.; Meskers, S. C. J.; Dekkers, H. P. J. M.; Meijer, E. W. *J. Am. Chem. Soc.* **1996**, *118*, 4908.
(29) Langeveld-Voss, B. M. W.; Christiaans, M. P. T.; Janssen, R. A. J.; Meijer, E. W. *Macromolecules* **1998**, *31*, 6702.
(30) Langeveld-Voss, B. M. W.; Janssen, R. A. J.; Meijer, E. W. *J. Mol. Struct.* **2000**, *521*, 285.
(31) Yashima, E.; Matsushima, T.; Okamoto, Y. *J. Am. Chem. Soc.* **1997**, *119*, 6345.
(32) Yashima, E.; Maeda, K.; Okamoto, Y. *Nature* **1999**, *399*, 449.
(33) Ishikawa, M.; Maeda, K.; Yashima, E. *J. Am. Chem. Soc.* **2002**, *124*, 7448.
(34) Berggren, M.; Bergman, P.; Fagerström, J.; Inganäs, O.; Andersson, M.; Weman, H.; Granström, M.; Stafström, S.; Wennerström, O.; Hjertberg, T. *Chem. Phys. Lett.* **1999**, *304*, 84.
(35) Nilsson, K. P. R.; Andersson, M. R.; Inganäs, O. *J. Phys.: Condens. Matter* **2002**, *14*, 10011.
(36) Sugimoto, R.; Takeda, S.; Gu, H. B.; Yoshino, K. *Chem. Exp.* **1986**, *1*, 635.
(37) Yoshino, K.; Hayashi, S.; Sugimoto, R. I. *Jpn. J. Appl. Phys* **1984**, *23*, L899.
(38) Jayakannan, M.; van Dongen, J. L. J.; Janssen, R. A. J. *Macromolecules* **2001**, *34*, 5386.
(39) Liu, J.; Loewe, R. S.; McCullough, R. D. *Macromolecules* **1999**, *32*, 5777.
(40) Abdou, M. S. A.; Lu, X.; Xie, Z. W.; Orfino, F.; Deen, M. J.; Holdcroft, S. *Chem. Mater.* **1995**, *7*, 631.
(41) McCarley, T. D.; Noble, C. O.; DuBois, C. J.; McCarley, R. L. *Macromolecules* **2001**, *34*, 7999.
(42) Demas, J.; Crosby, G. A. *J. Phys. Chem.* **1971**, *75*, 991−1024.
(43) Xu, C.; Webb, W. W. *J. Opt. Soc. Am. B* **1996**, *13*, 481.
(44) Sepaniak, M. J.; Yeung, E. S. *Anal. Chem.* **1977**, *49*, 1554.
(45) Wirth, M. J.; Fatunmbi, H. O. *Anal. Chem.* **1990**, *62*, 973.
(46) Pfeffer, W. D.; Yeung, E. S. *Anal. Chem.* **1986**, *58*, 2103.
(47) Nonlinear and Two-Photon Induced Fluorescence. In *Topics in Fluorescence Spectroscopy*; Lakowicz, J., Ed.; Plenum Press: New York, 1997; Vol. 5.
(48) Zipfel, W. R.; Williams, R. M.; Webb, W. W. *Nature Biotechnol.* **2003**, *21*, 1369.
(49) Norman, P.; Luo, Y.; Ågren, H. *Opt. Commun.* **1999**, *168*, 297.
(50) Wang, C. K.; Macak, P.; Luo, Y.; Ågren, H. *J. Chem. Phys.* **2001**, *114*, 9813.
(51) Beljonne, D.; Bredas, J. L. *J. Opt. Soc. Am. B* **1994**, *11*, 1380.

MA051188F